

# Recrystallization Kinetics of an Austenitic High-Manganese Steel Subjected to Severe Plastic Deformation

Zh. Ch. Yanushkevich<sup>a, \*</sup>, D. A. Molodov<sup>b</sup>, A. N. Belyakov<sup>a</sup>, and R. O. Kaibyshev<sup>a</sup>

<sup>a</sup>Belgorod State University, Belgorod, 308015 Russia

<sup>b</sup>Rheinisch-Westfälische Technische Hochschule Aachen University, Aachen, 52074 Germany

\*e-mail: yanushkevich@bsu.edu.ru

Received April 4, 2016

**Abstract**—The evolution of the microstructure and the properties of an austenitic high-manganese steel subjected to severe deformation by cold rolling and subsequent recrystallization annealing is investigated. Cold rolling is accompanied by mechanical structural twinning and shear banding. The microhardness and microstructural analysis of annealed samples are used to study the recrystallization kinetics of the high-manganese steel. It is shown that large plastic deformation and subsequent annealing result in rapid development of recrystallization processes and the formation of an ultrafine-grained structure. A completely recrystallized structure with an average grain size of 0.64  $\mu\text{m}$  forms after 30-min annealing at a temperature of 550°C. No significant structural changes are observed when the annealing time increases to 18 h, which indicates stability of the recrystallized microstructure. The steel cold rolled to 90% and annealed at 550°C for 30 min demonstrates very high strength properties: the yield strength and the tensile strength achieve 650 and 850 MPa, respectively. The dependence of the strength properties of the steel on the grain size formed after rolling and recrystallization annealing is described by the Hall–Petch relation.

DOI: 10.1134/S0036029516090184

## INTRODUCTION

The modern trends in the automobile industry require reducing the automobile weight and the fuel consumption and increasing the vehicle safety significantly. Thus, the importance of the works dedicated to the study and development of new high-strength and plastic structural materials is beyond question. High-manganese steels with TWIP (twinning induced plasticity) are among the promising next-generation high-strength steels [1–4]. The mechanical behavior and the strain hardening of these steels greatly depend on the stacking fault energy, which is responsible for the activation energy of a deformation mechanism. It is known from available published data that high-strength TWIP steels have a low stacking fault energy in the range 15–30  $\text{mJ}/\text{m}^2$  [5, 6]. TWIP steel with the chemical composition Fe–0.3C–17Mn–1.5Al, which is studied here, belongs to this class.<sup>1</sup> These steels possess a high plasticity and strain hardening, which make them promising for a wide application as structural materials. However, the use of steels of this class is constrained by a relatively low yield strength, which is the main disadvantage of hot-rolled semifinished high-manganese austenitic steels [2, 7]. Providing a significant increase in the strength properties, cold

plastic deformation is the simplest and most common way among the existing methods to enhance the strength properties of structural steels and alloys. The yield strength of high-manganese TWIP steels can be improved to 1.5 GPa using large plastic deformation [8, 9]. The hardening can be enhanced by deformation twinning (leading to structural hardening according to the Hall–Petch law) and the hardening due to the deformation-induced dislocation density growth [10–12]. However, an increase in the strength in this case is accompanied by a decrease in the plasticity. At a sufficiently high retained level of strength, plasticity can be increased by forming an ultrafine-grained structure, for example, by special-purpose heat treatment, which includes deformation and annealing [13–15]. Such heat treatment allows a microstructure with an average grain size in the range 1–10  $\mu\text{m}$  to be formed. The application of large deformation allows the formation of grains with a size below 1  $\mu\text{m}$  [16]. Thus, information on the effect of the degree of deformation, the temperature, and the postdeformation annealing time on structural changes is necessary to fabricate semifinished products with an ultrafine-grained structure and the desired grain size, which determines the mechanical properties of high-manganese steels.

The aim of the present work is to investigate the recrystallization kinetics of an austenitic high-manga-

<sup>1</sup> Hereafter, the element contents are given in wt %.

nese Fe–0.3C–17Mn–1.5Al steel subjected to large plastic deformation and subsequent annealing. The work is focused on the influence of the recrystallization annealing time on the microstructure and mechanical properties of the steel.

## EXPERIMENTAL

An ingot of a high-Mn austenitic TWIP steel containing (wt %) 0.3 C, 17.7 Mn, 1.5 Al, 0.01 Si, 0.07 Cr, 0.007 S, and 0.02 P was investigated. Initial workpieces to be deformed by cold rolling to a strain of 90 and 95% were cut from the hot-rolled steel ingot annealed at 1150°C for 4 h. The deformed samples of the initial workpieces were annealed at 550°C for various periods of time (from 20 s to 18 h).

The microstructural investigations of the austenitic high-manganese steel subjected to rolling and annealing were performed in the longitudinal section of the samples using an Olympus GX71 optical microscope, a Quanta Nova Nanosem 450 scanning electron microscope (SEM) equipped with a detector for electron backscatter diffraction (EBSD), and a Jeol JEM-2000 transmission electron microscope (TEM). Samples for structural examination were electropolished using an electrolyte composed of 10% HClO<sub>4</sub> and 90% CH<sub>3</sub>COOH at a voltage of 20 V and room temperature. The samples were etched in a solution consisting of 2 g K<sub>2</sub>S<sub>2</sub>O<sub>5</sub> and 100 mL saturated Klemm I solution (Na<sub>2</sub>S<sub>2</sub>O<sub>3</sub> + 5H<sub>2</sub>O). Misorientation maps (EBSD maps) were built with the TSL OIM Analysis software designed for processing backscattered electron images. The average grain size was calculated by the random linear intercept method taking into account only high-angle boundaries with the minimum misorientation angle of 15°, including the boundaries of annealing twins.

Vickers microhardness  $HV_{0.2}$  was measured on a 402 MVD hardness tester at a load of 2 N. Tensile tests were carried out with an Instron 5882 universal testing machine on samples with a gauge portion of 1.5 × 3 × 16 mm cut out along the rolling direction. Yield strength  $\sigma_{0.2}$ , ultimate tensile strength  $\sigma_u$ , and relative elongation  $\delta$  were determined from the tensile tests performed at room temperature and a strain rate of 2 mm/min.

## RESULTS AND DISCUSSION

### *Deformed Microstructure*

Metallographic studies showed that the initial microstructure of the austenitic high-manganese TWIP Fe–0.3C–17Mn–1.5Al steel was quite uniform and composed of austenitic grains with an average size of 24  $\mu\text{m}$  and annealing twins (Fig. 1a).

The typical microstructures formed in the steel after cold working to 90 and 95% at room temperature are shown in Figs. 1b and 1c. Cold working is accom-

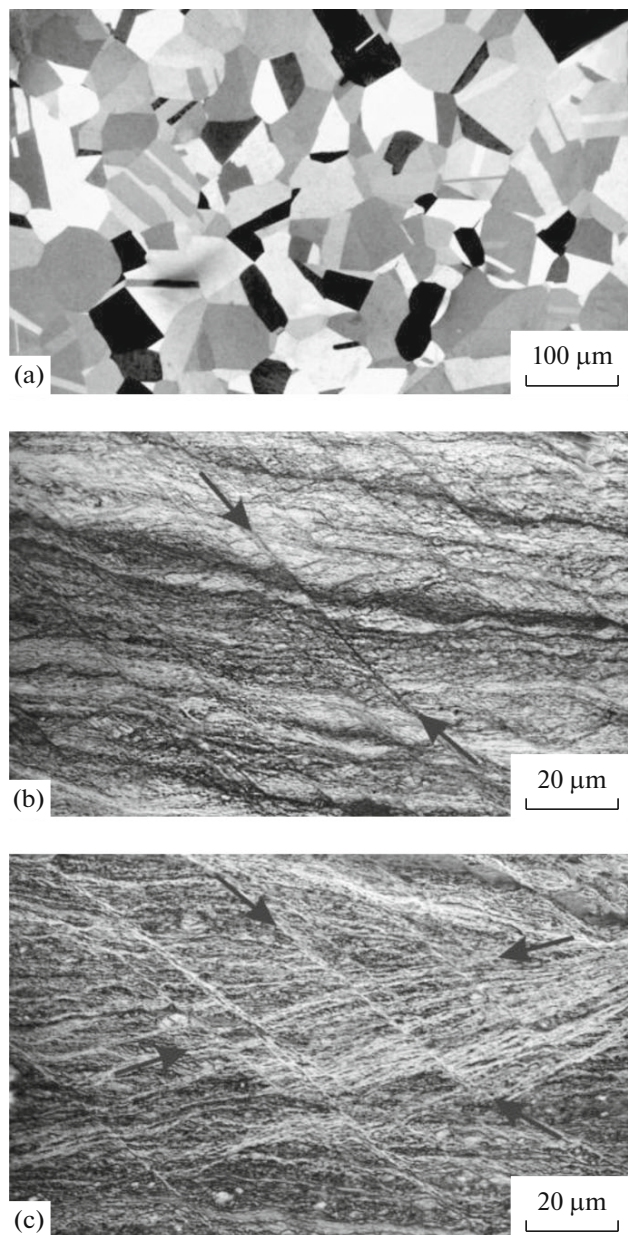


**Fig. 1.** Microstructure of high-manganese TWIP steel (a) in the initial state and after cold rolling to a strain of (b) 90 and (c) 95%.

panied by deformation twinning, which results in the formation of a deformation microstructure with a high density of twins [8, 17]. Large plastic deformation (to 90%) causes the formation of a system of local shear microbands (indicated by arrows in Fig. 1b), which cross twinned grains in the entire volume of the deformed samples. The number of such shear microbands increases with the strain up to 95% (Fig. 1c).

The deformation microstructure consists of islands of nanotwins surrounded by shear microbands (indicated by arrows). There are two families of intersected shear microbands. Commonly, microbands are

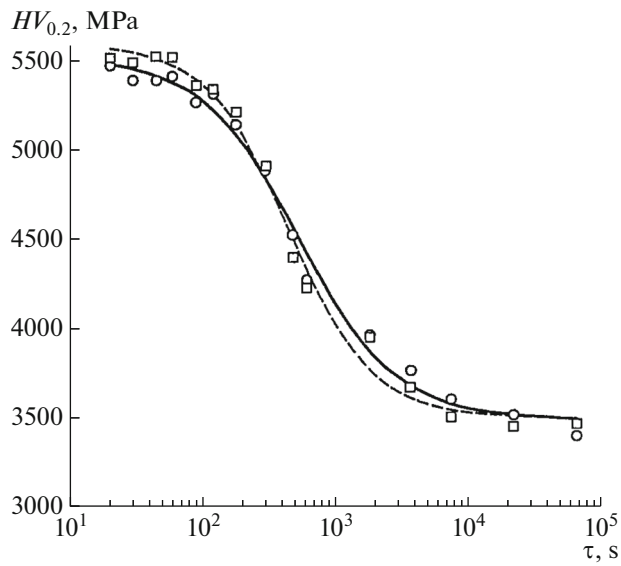


**Fig. 2.** Microhardness  $HV_{0.2}$  of the cold-rolled Fe–0.3C–17Mn–1.5Al steel vs. annealing time  $\tau$  at a strain of (○) 90 and (□) 95%.

located along the planes of the maximum tangential stresses. The shear microbands resulted from 95% deformation are located at an angle of  $40^\circ$  to the rolling plane.

Cold rolling significantly increases the strength properties, which is related to the unique property of TWIP steel to be strain hardened. The hardness of the steel rolled to 95% increases from 1510 to 5600 MPa. The strength increases after rolling due to a high dislocation density, the formation of deformation twins, and a high density of shear microbands [3, 18].

### Recrystallization Annealing

The intensity of softening processes in the austenitic high-manganese Fe–0.3C–17Mn–1.5Al steel subjected to large plastic deformation and subsequent annealing can be estimated from the change in its microhardness (Fig. 2). The microhardness decreases gradually with the annealing time, and the steel undergoes a number of structural changes to be divided into recovery and recrystallization processes. Short-term annealing (from 20 to 45 s) changes the microhardness insignificantly because of the stages of recovery and the onset of recrystallization. An increase in the annealing time from 45 s to 10 min results in an abrupt decrease in the hardness from 5500 to 4230 MPa. In this annealing time range, recrystallization processes develop intensely. The microhardness decreases to 3965 MPa as the annealing time increases to 30 min. No significant changes in the microhardness are observed when the annealing time increases to 18 h.

Figure 3 presents the fine structure of the steel cold rolled to 95% and subsequently annealed at  $550^\circ\text{C}$  for a short period of time (45 s–10 min). The microstructure after short-term annealing for 45 s is characterized by fine dislocation-free grains  $\sim 0.3 \mu\text{m}$  in size, which can be considered as recrystallization nuclei (Fig. 1a). It is known that a large amount of the energy stored during deformation increases the driving force of recrystallization; therefore, we can observe the formation of new grains in a short period of annealing time. An increase in the annealing time to 2 min results in a great number of fine recrystallized grains. In this case, the microstructure consists of regions of severely deformed matrix, which alternate with recrystallization grains. The size of recrystallized grains changes from 50 to 500 nm. The fraction of recrystallized

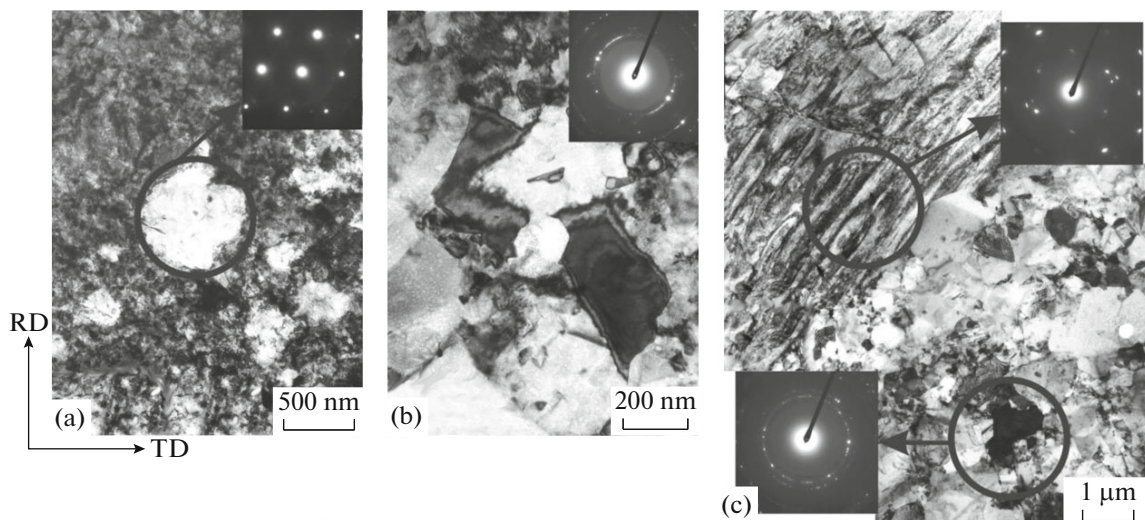


**Fig. 3.** Fine structure of the high-manganese steel after cold rolling to 95% and subsequent annealing at  $550^\circ\text{C}$  for (a) 45 s, (b) 2 min, and (c) 8 min: structure in the rolling direction (RD) and in the transverse direction (TD).

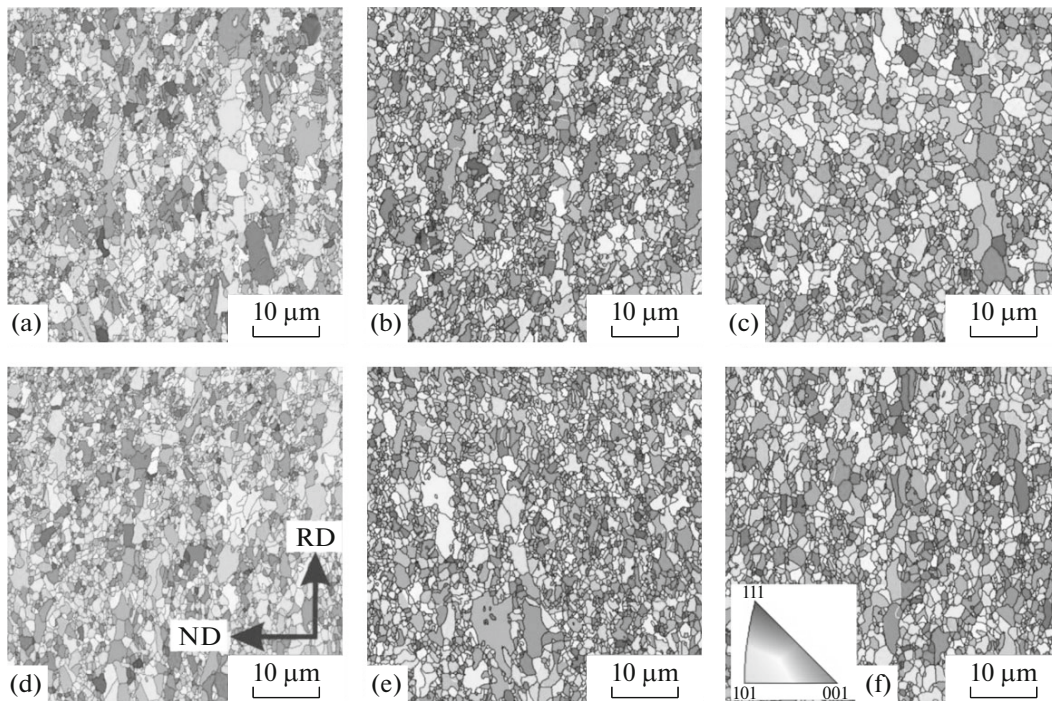


**Fig. 4.** Microstructure of the steel after cold deformation at various strains  $\varepsilon$  and subsequent annealing for various periods of time  $\tau$  at 550°C: (a–c)  $\varepsilon = 90\%$ ,  $\tau = 30$  min, 1 h, and 2 h, respectively; (d–f)  $\varepsilon = 95\%$ ,  $\tau = 30$  min, 1 h, and 2 h, respectively. Structure in the rolling direction (RD) and in the direction normal to the rolling plane (ND).

grains increases when the annealing time increases to 8 min; the size of these grains is 0.4  $\mu\text{m}$ .

Figure 4 shows the microstructure of the Fe–0.3C–17Mn–1.5Al steel after rolling to a degree of 90–95% and annealing for a time from 30 min to 2 h. Annealing carried out for 30 min leads to complete replacement of the deformation microstructure by a recrystallized one with an average grain size of 0.64–0.65  $\mu\text{m}$  at  $\varepsilon = 90$ –95%, respectively. The recrystallized microstructure contains fine equiaxed grains and coarse grains elongated in the rolling direction. Such nonuniformity can be attributed to the presence of structural elements such as twins and shear microbands in the deformed microstructure, which then results in a nonuniform distribution of recrystallization nuclei.

An increase in the annealing time to 2 h does not cause a noticeable increase in the average grain size. The grain size in the steel deformed to  $\varepsilon = 90$  and 95% is within 1  $\mu\text{m}$ . An analysis of the microstructure formed after large plastic deformation and subsequent recrystallization annealing shows that the previous deformation weakly affects the recrystallized microstructure.

Figure 5 presents the steel microstructure formed after cold working to 90–95% and subsequent prolonged annealing at 550°C for  $\tau = 6$ –18 h. No significant differences from the microstructure formed upon shorter annealing (from 30 min to 2 h) are observed.

The grain size slightly increases from 0.87 to 0.98  $\mu\text{m}$  at a strain of 90% and from 0.75 to 0.83  $\mu\text{m}$  at 95% when the annealing time increases from 6 to 18 h.

The kinetics of structural changes upon annealing can be estimated using the rate of softening [19]. Figure 6 depicts the fraction of softening as a function of the annealing time for the Fe–0.3C–17Mn–1.5Al steel subjected to cold rolling and subsequent annealing. The fraction of softening for the TWIP steel after annealing was calculated from the following equation [20]:

$$X = (HV_{0.2}^{\varepsilon} - HV_{0.2}^t) / (HV_{0.2}^{\varepsilon} - HV_{0.2}^0), \quad (1)$$

where  $HV_{0.2}^{\varepsilon}$ ,  $HV_{0.2}^t$ , and  $HV_{0.2}^0$  are the microhardnesses of the samples after deformation, annealing, and full recrystallization, respectively. According to microstructure examination, a completely recrystallized structure forms after annealing for 30 min:  $HV_{0.2}^0 = 3964$  MPa after deformation to 90% and  $HV_{0.2}^0 = 3956$  MPa after deformation to 95%. The curve in Fig. 6 suggests that, after short-term annealing (20–90 s), the fraction of softening is less than 10%, which corresponds to the stage of recovery (incubation time of recrystallization). Rapid softening, which corresponds to intense recrystallization, is observed when the annealing time is increased to 30 min. After 30-min annealing at 550°C, the fraction of softening reaches 100% and corresponds to a fully recrystallized microstructure.

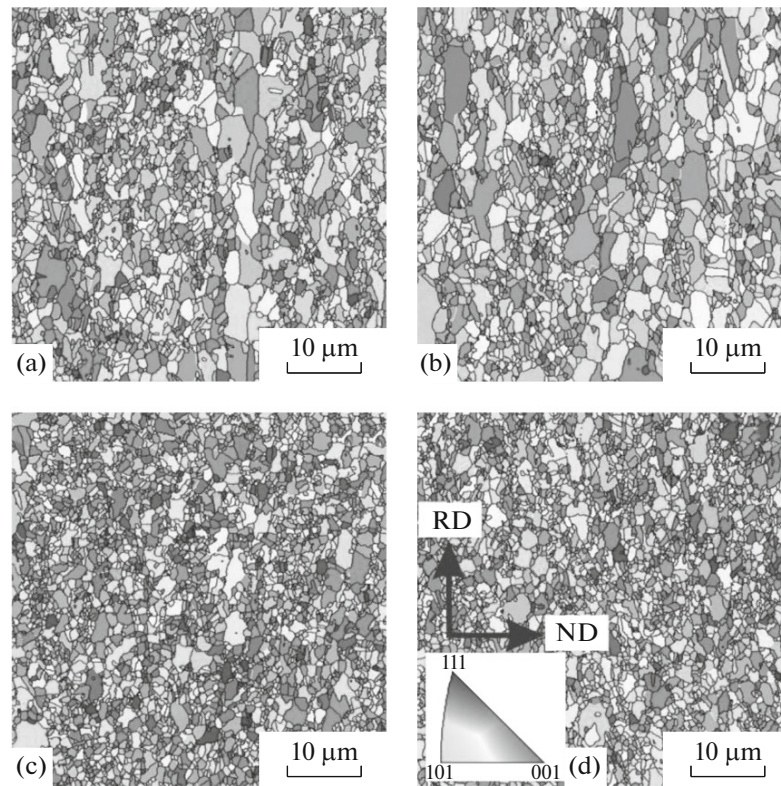


**Fig. 5.** Microstructure of the steel after cold deformation to various strains  $\varepsilon$  and subsequent prolonged annealing for  $\tau$  at 550°C: (a, b)  $\varepsilon = 90\%$ ,  $\tau = 6$  and 18 h, respectively; (c, d)  $\varepsilon = 95\%$ ,  $\tau = 6$  and 18 h, respectively.

The effect of the annealing time on the grain size in the Fe–0.3C–17Mn–1.5Al steel after cold rolling and subsequent recrystallization annealing can be estimated from Fig. 7.

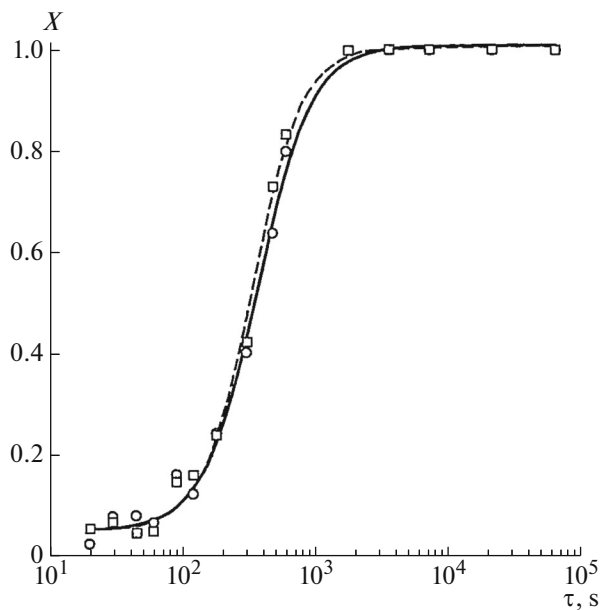


**Fig. 6.** Effect time  $\tau$  of annealing at 550°C on the fraction of softening  $X$  in the Fe–0.3C–17Mn–1.5Al steel after cold rolling to a strain of (○) 90 and (□) 95%.

The resulting dependence of average grain size  $D$  can be described as a power function of the annealing time,  $D \sim \tau^{1/n}$ , where  $n$  is the grain growth exponent. The curve in Fig. 6 suggests that the microstructure remains stable during 18-h annealing; the grain size increases from 0.65 to 0.98  $\mu\text{m}$  at a strain of 90%. The microstructure of recrystallization of the samples rolled to 95% is characterized by rather high thermal stability. The grain growth exponent of the samples

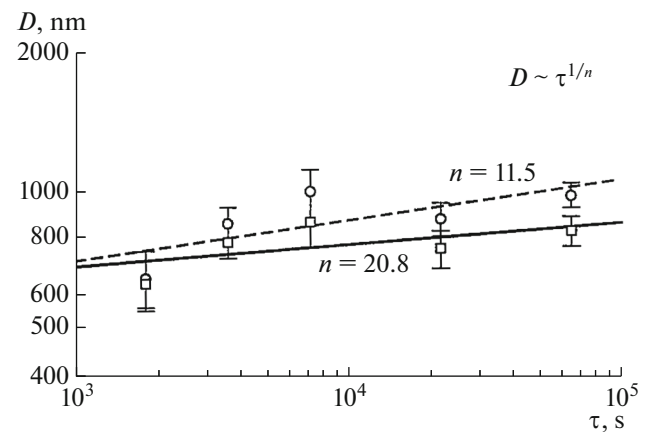


**Fig. 7.** Recrystallized grain size  $D$  of the high-Mn steel after rolling and annealing as a function of annealing time  $\tau$ .

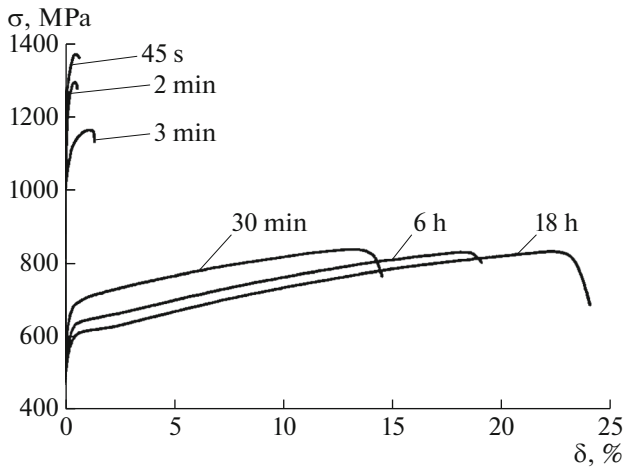


**Fig. 8.** Uniaxial tensile stress–strain diagrams obtained at room temperature for the high-manganese steel after cold rolling ( $\epsilon = 90\%$ ) and recrystallization annealing at  $550^\circ\text{C}$  for various annealing times (numerals at the curves).

deformed to 95% is  $n = 20.8$ , and we have  $n = 11.5$  for the samples rolled to 90%. The deceleration and subsequent decay of recrystallization processes are related to the termination of the growth of recrystallized grains touching each other.

*Mechanical Properties*

Figure 8 shows the uniaxial tensile stress-strain diagrams obtained at room temperature for the high-manganese steel after rolling to 90% and recrystallization annealing at  $550^\circ\text{C}$ .

An increase in the annealing time causes a decrease in the strength and an increase in the plasticity: the ultimate tensile strength decreases from 1370 to 830 MPa and the relative elongation increases from 0.63 to 24% when the annealing time is increased from 45 s to 18 h. It should be noted that an increase in the annealing time from 30 min to 18 h slightly affects the processes developing in the structure and exerts no effect on the properties of the steel.

The yield strength changes weakly in the annealing time range from 30 min to 18 h due to microstructural stability. The tensile stress-strain diagrams obtained after short-term annealing for a time from 45 s to 8 min have no stage of steady elongation, and the relative elongation is within 0.63–1.36%. Such behavior can be explained by the presence of a great fraction of a residual deformed microstructure and a high density of defects in the structure. The presence of such structural elements as shear bands and deformation twins and a high dislocation density lead to rapid localization of plastic flow and material fracture. The mechanical properties of the steel after uniaxial tensile tests performed at room temperature are listed in the table.

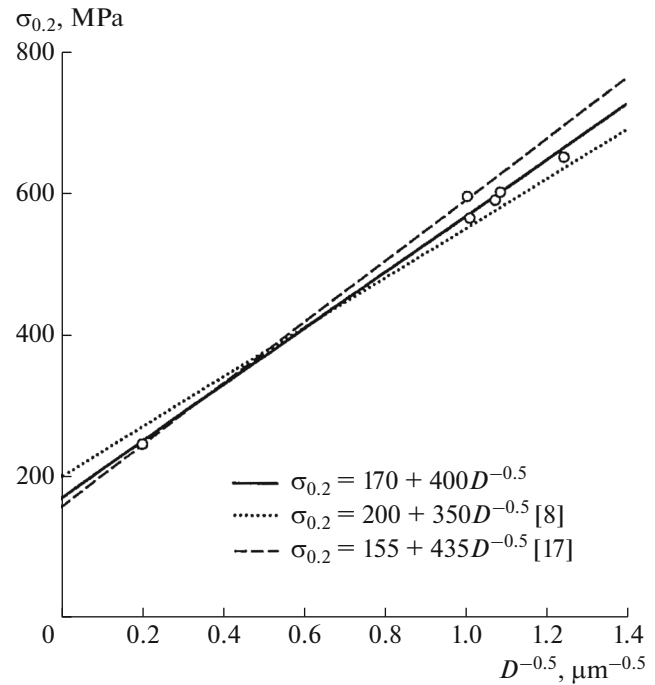


**Fig. 9.** Yield strength vs. the average grain size of the Fe–0.3C–17Mn–1.5Al steel cold rolled to a strain of 90% and annealed at  $550^\circ\text{C}$ : (—) this work, (····) [8], and (---) [17].

The grain size strongly affects yield strength  $\sigma_{0.2}$ . The structural hardening of the Fe–0.3C–17Mn–1.5Al steel samples subjected to cold rolling to a strain of 90% and annealing at  $550^\circ\text{C}$  can be described by the dependence of yield strength  $\sigma_{0.2}$  on grain size  $D$ .

Such an experimental dependence is shown in Fig. 9 and described by the Hall–Petch relation,

$$\sigma_{0.2} = \sigma_0 + K_y D^{-0.5}, \quad (2)$$

Effect of annealing time  $\tau$  on the strength and plasticity properties of the Fe–0.3C–17Mn–1.5Al steel subjected to cold rolling to a strain of 90% and annealing at  $500^\circ\text{C}$

$\tau$	$\sigma_{0.2}$	$\sigma_u$	$\delta, \%$
	MPa		
45 s	1310	1370	0.63
2 min	1240	1290	0.61
8 min	1080	1160	1.36
30 min	650	840	14.5
1 h	600	850	8.0
2 h	595	760	13.5
6 h	590	830	19.0
18 h	565	830	24.0

where  $\sigma_0 = 170$  MPa and  $K_y = 400$  MPa  $\mu\text{m}^{0.5}$ . For comparison, similar dependences for other austenitic high-Mn steels with various compositions after various treatments are shown in Fig. 9 [8, 17, 21–23]. Despite some differences in the chemical compositions, the steels exhibit nearly the same behavior of the curves, and the values of such main parameters as  $\sigma_0$  and  $K_y$  are in the range 155–170 MPa and 350–435 MPa  $\mu\text{m}^{0.5}$ , respectively.

## CONCLUSIONS

(1) Severe plastic deformation of a high-manganese Fe–0.3C–17Mn–1.5Al steel to 90–95% is accompanied by the formation of numerous deformation twins and shear microbands, resulting in significant hardening. The hardness of the steel increases from 1510 to 5600 MPa after rolling to a strain of 95%.

(2) Short-term annealing (45–90 s) at 550°C weakly changes the hardness, whereas an increased annealing time (to 30 min) results in a sharp softening, which can be explained by intense recrystallization processes. The microstructure after 30-min annealing is completely recrystallized and the average grain size is 0.64  $\mu\text{m}$ . No significant microstructural changes are observed with an increase in the annealing time to 18 h, which indicates stability of the recrystallized microstructure.

(3) The annealing-time dependence of the average grain size can be described as a power function  $D \sim \tau^{1/n}$ , where grain growth exponent  $n$  changes from 11.5 to 20.8 when the strain is increased from 90 to 95%.

(4) Uniaxial tensile tests performed at room temperature showed that an increase in the annealing time results in a decrease in the strength and an increase in the plasticity. The ultimate tensile strength decreases from 1370 to 830 MPa and the relative elongation increases from 0.63 to 24% when the annealing time increases from 45 s to 18 h.

(5) It was established that grain boundaries mainly contribute to the hardening of the fully recrystallized steel; therefore, the yield strength of the steel after recrystallization annealing as a function of the average grain size can be described by the Hall–Petch relation  $\sigma_{0.2} = \sigma_0 + K_y D^{-0.5}$ , where  $\sigma_0 = 170$  MPa and  $K_y = 400$  MPa  $\mu\text{m}^{0.5}$ .

## ACKNOWLEDGMENTS

This work was supported by the Ministry of Education and Science of the Russian Federation, project no. 14.578.21.0069 RFMEFI57814X0069.

## REFERENCES

- H. Hofmann, D. Mattissen, and T. W. Schaumann, “Advanced cold rolled steels for automotive applications,” *Mater. Werkst.* **37**, 716–723 (2006).
- O. Bouaziz, S. Allain, C. P. Scott, P. Cugy, and D. Barbier, “High manganese austenitic twinning induced plasticity steels: A review of the microstructure properties relationships,” *Curr. Opin. Solid State Mater. Sci.* **15**, 141–168 (2011).
- C. Haase, S. G. Chowdhury, L. A. Barrales-Mora, D. A. Molodov, and G. Gottstein, “On the relation of microstructure and texture evolution in an austenitic Fe–28Mn–0.28C TWIP steel during cold rolling,” *Met. Mater. Trans. A* **44**, 911–922 (2013).
- V. Shterner, A. Molotnikov, I. Timokhina, Y. Estrin, and H. Beladi, “A constitutive model of the deformation behaviour of twinning induced plasticity (TWIP) steel at different temperatures,” *Mater. Sci. Eng. A* **613**, 224–231 (2014).
- S. Allain, J.-P. Chateau, O. Bouaziz, S. Migot, and N. Guelton, “Correlations between the calculated stacking fault energy and the plasticity mechanisms in Fe–Mn–C alloys,” *Mater. Sci. Eng. A* **387**, 158–162 (2004).
- A. Dumay, J.-P. Chateau, S. Allain, S. Migot, and O. Boueiziz, “Influence of addition elements on the stacking-fault energy and mechanical properties of an austenitic Fe–Mn–C steel,” *Mater. Sci. Eng. A* **483**, 184–187 (2008).
- O. Grässel, L. Krüger, G. Frommeyer, and L. W. Meyer, “High strength Fe–Mn–(Al, Si) TRIP/TWIP steels development—properties—application,” *Int. J. Plast.* **16**, 1391–1409 (2000).
- P. Kusakin, A. Belyakov, C. Haase, R. Kaibyshev, and D. A. Molodov, “Microstructure evolution and strengthening mechanisms of Fe–23Mn–0.3C–1.6Al TWIP steel during cold rolling,” *Mater. Sci. Eng. A* **617**, 52–60 (2014).
- Z. Yanushkevich, A. Belyakov, R. Kaibyshev, C. Haase, and D.A. Molodov, “Structural/textural changes and strengthening of an advanced high-Mn steel subjected to cold rolling,” *Mater. Sci. Eng. A* **651**, 763–773 (2016).
- R. W. Armstrong, “60 years of Hall–Petch: past to present nano-scale connections,” *Mater. Trans.* **56**, 2–12 (2014).
- N. Hansen, “Hall–Petch relation and boundary strengthening,” *Scr. Mater.* **51**, 801–806 (2004).
- E. O. Hall, “The deformation and ageing of mild steel: III discussion of results,” *Proc. Phys. Soc., Sect. B* **64**, 747 (1951).
- Y. Wang, M. Chen, F. Zhou, and E. Ma, “High tensile ductility in a nanostructured metal,” *Nature* **419**, 912–915 (2002).
- N. Tsuji, N. Kamikawa, R. Ueji, N. Takata, H. Koyama, and D. Terada, “Managing both strength and ductility in ultrafine grained steels,” *ISIJ Inter.* **48**, 1114–1121 (2008).
- Z. Zhang, D. Orlov, S.K. Vajpai, B. Tong, and K. Ameyama, “Importance of bimodal structure topology in the control of mechanical properties of a stainless steel,” *Adv. Eng. Mater.* **17**, 791–795 (2015).
- R. Saha, R. Ueji, and N. Tsuji, “Fully recrystallized nanostructure fabricated without severe plastic deformation in high-Mn austenitic steel,” *Scr. Mater.* **68**, 813–816 (2013).

17. Z. Yanushkevich, A. Belyakov, R. Kaibyshev, C. Haase, and D. A. Molodov, "Effect of cold rolling on recrystallization and tensile behavior of a high-Mn steel," *Mater. Charact.* **112**, 180–187 (2016).
18. Z. Yanushkevich, A. Belyakov, R. Kaibyshev, and D. Molodov, "Effect of large plastic deformation on microstructure and mechanical properties of a TWIP steel," *IOP Conf. Ser. Mater. Sci.* **63**, 12064 (2014).
19. I. Shakhova, V. Dudko, A. Belyakov, K. Tsuzaki, and R. Kaibyshev, "Effect of large cold rolling and subsequent annealing on microstructure and mechanical properties of an austenitic stainless steel," *Mater. Sci. Eng. A* **545**, 176–186 (2012).
20. A. Belyakov, K. Tsuzaki, Y. Kimura, and Y. Mishima, "Annealing behavior of a ferritic stainless steel subjected to large-strain cold working," *J. Mater. Res.* **22**, 3042–3051 (2007).
21. K. Jeong, J.-E. Jin, Y.-S. Jung, S. Kang, and Y.-K. Lee, "The effects of Si on the mechanical twinning and strain hardening of Fe–18Mn–0.6C twinning-induced plasticity steel," *Acta Mater.* **61**, 3399–3410 (2013).
22. J.-E. Jin and Y.-K. Lee, "Strain hardening behavior of a Fe–18Mn–0.6C–1.5 Al TWIP steel," *Mater. Sci. Eng. A* **527**, 157–161 (2009).
23. I. Gutierrez-Urrutia and D. Raabe, "Multistage strain hardening through dislocation substructure and twinning in a high strength and ductile weight-reduced Fe–Mn–Al–C steel," *Acta Mater.* **60**, 5791–5802 (2012).

*Translated by T. Gapontseva*